Time-Resolved Pulsed Spray Drop Sizing at Elevated Pressures

J. A. Drallmeier* and J. E. Peters†
University of Illinois at Urbana-Champaign, Urbana, Illinois

An experimental program was conducted to measure drop sizes in pulsed sprays for diesel and fuel-injected spark ignition engine applications. A forward-scattering unit was designed with a high-speed data acquisition system to permit the measurement of drop sizes in sprays at 0.4-ms intervals. Data were taken at elevated pressures from 0.345 to 3.45 MPa with a 0-deg pintle nozzle. The Sauter Mean Diameter (SMD) and size distribution were calculated using a computational method that is independent of a predetermined distribution function. Results taken at the spray centerline indicate that for most elevated pressures, the SMD in the secondary injection region tended to increase as the pressure in the fuel line decreased and tended to increase with increasing environmental pressure, both suggesting an inverse relationship between drop size and the pressure drop across the nozzle. Also as the environmental pressure was raised, the distribution width decreased at a slower rate than the SMD increased, indicating a spreading of the drop sizes with injection time at elevated pressures. Significant cycle-to-cycle variation in both the SMD and distribution width indicate that cycle-to-cycle variations must be considered in pulsed sprays. In addition, more variation was seen between random rather than consecutive cycles.

Nomenclature

D = drop diameter
I = intensity
I_0 = intensity at the zero scattering angle
J_1 = Bessel function of the first kind of order 1
$N(\alpha)$ = number distribution of particles
α = dimensionless size parameter, $=\pi D/\lambda$
γ = undetermined multiplier
θ = scattering angle
λ = wavelength of light

Introduction

IN liquid spray combustion system such as diesels, fuel-injected spark ignition engines, furnaces, and gas turbines, the characteristics of the fuel spray are important to the combustion process. Many studies have shown the effect of drop size on ignition, burning rate of fuel-air mixtures, flame structure, and mixing. From these studies, it is clear that the knowledge of fuel drop size behavior in a spray would be advantageous in the analysis of spray combustion and for improving practical injection systems. In response to this need, several drop size measurement techniques have been developed.

Papers, such as those by Jones,[1] Azzopardi,[2] McCreath and Beer,[3] and Hirleman,[4] present reviews of the various measurement techniques available. The techniques can be broken down into the three main categories of electrical, mechanical, and optical methods. A large advantage of optical methods over the others is that they are nonintrusive and, therefore, do not affect the flowfield of study. Optical methods can be further broken down into imaging methods, ensemble multiparticle methods, and single particle counters. Of the ensemble multiparticle methods, the forward-scattering method was chosen for this work because of its relative low cost and proven capabilities in analyzing fuel sprays. The forward-scattering technique, as described by Swithenbank et al.,[5] utilizes the scattering of light in the forward direction by the drops in the spray. The shape of the resulting scattered light intensity profile provides the necessary information to determine the sizes and distributions. This technique has been used by several investigators primarily to study continuous sprays suitable for gas-turbine or furnace applications, but few have looked at pulsed sprays.

The forward-scattering technique has been used by Chigier[6] to obtain some preliminary results for mean drop size in pulsed diesel sprays. Peters and Mellor[7] also used this technique to measure the mean drop size in a pulsed fuel spray with a relatively long injection time of about 28 ms. They combined the results from several different cycles to obtain time-resolved information for a standard cycle.

Recently, Sangeorzan et al.[8] measured the mean drop size and size distributions in pulsed diesel sprays in an ambient pressure environment using the forward-scattering technique. They were unable, however, to make measurements through the entire spray (edge to edge) due to large laser beam attenuation values at the spray centerline. The large attenuation measurements indicate the possibility of multiple scattering effects.

While these studies show conclusively that a forward-scattering measurement system is capable of measuring mean drop sizes and drop size distributions in pulsed fuel sprays, they provided insufficient detailed time-resolved data. In particular, little, if any, published data can be found showing the time-resolved effects of ambient pressure on drop sizes. The pulsed spray work of Hiroyasu and Kadota[9] using a liquid immersion technique and Takeuchi et al.[10] using microphotography have looked at the effects of ambient pressure, but only by taking measurements from different cycles at different injection times and combining the results to obtain one standard cycle. It is the goal of this program to provide detailed, time-resolved, measurements of the mean drop size and drop size distribution using the forward-scattering technique during the course of single injection cycles at varying ambient pressure conditions looking at both consecutive and random cycles.

Received Aug. 20, 1985; revision received Dec. 12, 1985.

*Graduate Research Assistant, Department of Mechanical and Industrial Engineering.
†Assistant Professor, Department of Mechanical and Industrial Engineering. Member AIAA.

Experimental Program

Experimental Apparatus

The experimental setup consists of a spray tunnel and fuel, optical, and data acquisition systems. The spray tunnel is a blowdown-type wind tunnel with variable pressure and flow rate in which the fuel injector is mounted as shown in Fig. 1. A low continuous flow (variable from 0.004 to 0.20 kg/s) is desired during tunnel testing to prevent the accumulation of the fuel spray. In order to simulate conditions found in a diesel engine, the spray tunnel can be pressurized up to 3.4 MPa using two compressed nitrogen tanks. The sudden expansion of the nitrogen from the tanks to working pressure of the spray tunnel required that heaters be installed in the supply line to heat the nitrogen to room temperature.

The spray tunnel itself is constructed of a 17.8-cm-o.d. by 10.2-cm-i.d. seamless steel tube with a wall thickness of 3.8 cm. Such a large wall thickness was chosen to ease the design of the window mounts. On the top of the tunnel, as seen in Fig. 1, a steel end cap is bolted to the flange and provides inlet holes for the nitrogen supply, fuel injector line, and thermocouple. On the other end of the tunnel, a 180-deg elbow is used as a trap for the fuel from the fuel injector. Various-sized exit orifice plugs can be installed in the end cap to provide different tunnel velocities. From the exit orifice the fuel vapor/nitrogen mixture is exhausted via an exhaust duct.

Three optical access ports are provided in the spray tunnel. The quartz inlet windows (inlet for laser beam) are 3.8 cm in diameter and 1.59 cm thick and the quartz outlet windows, to allow the diffracted light to leave, are 6.4 cm in diameter and 2.54 cm thick. Caps are placed over the windows to hold them in place. The cap for the exit window has an inside radius of 2.54 cm. This exit opening is large enough to allow all diffracted light through that is within the first intensity minimum for a 3.5-μm particle located nearest the inlet window.

The diesel fuel injector is located in the center of the spray tunnel and has both horizontal and vertical movement. The injector used in the spray tunnel was a Bosch HSM 780519 nozzle holder with a NPM 770073 nozzle with stock opening pressure of 12 MPa. This is a 0-deg pintle nozzle of the type that has been used on the International Harvester 6.9-liter engine. The fuel-line pressure is monitored by a Kistler Model 607F122 piezoelectric-type pressure transducer installed in the fuel line. The fuel pump is a Bosch Type APE-B single-cylinder, in-line pump with a maximum speed of 1300 rpm. Finally, a trigger mechanism which outputs a 5-V pulse at the beginning of the fuel injection was constructed that initiates the data acquisition sampling program.

The optical system shown schematically in Fig. 2 makes use of the forward-scattering technique for the measurement of drop size distributions. This technique requires that a collimated beam be passed through the spray and then the angular distribution of scattered energy be measured. The energy measurements are combined with the equations from diffraction theory to obtain the drop size distribution in the spray.

The light source is a 4-mW He-Ne laser. The output from this laser is conditioned by passing the beam through a spatial filter which eliminates noise from the intensity profile. Once through the spatial filter, the beam is collimated using a convex collimating lens to a $1/e^2$ diameter of 6 mm. Now the beam is ready to be passed into the fuel spray in the spray tunnel via the inlet quartz optical access window. The beam scatters from the drops and the forward diffracted light exits through the outlet quartz window. A Fourier transform lens is used to collect the diffracted light and to form a Fraunhofer diffraction pattern of the drop distribution. This transform or collecting lens has a 300-mm focal length and a photodetector was placed at its focal plane.

The photodetector used is manufactured by Recognition Systems and consists of a silicon wafer with 32 concentric

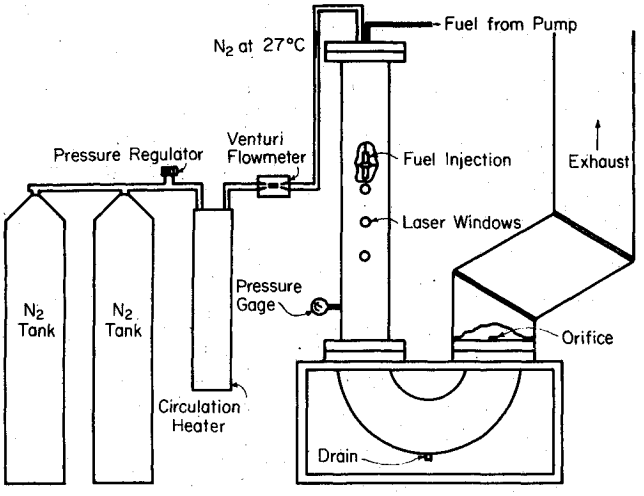

Fig. 1 Pulsed spray experimental apparatus.

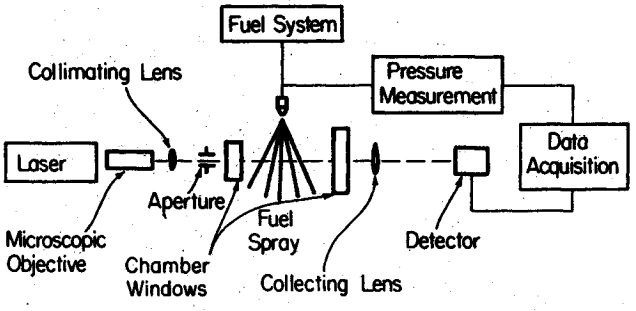

Fig. 2 Pulsed spray optical system.

half-ring elements. The scattered energy profile measured by the photodetector was sampled by a Digital Equipment Corporation PDP 1134/A computer. The computer has a total of 16 input channels and has been fitted with a Data Translation analog-to-digital (A/D) converter. Since there are only 16 input channels, 14 of the 32 output channels from the photodetector and the pressure transducer output are recorded. Output channels (or rings) 13 to 20 and even rings 22 to 32 were sampled since the first 12 rings registered artificially high energy values due to crosstalk. The unscattered energy signal created sufficient saturation to affect these first 12 rings. As will be discussed subsequently, the data from the sampled rings were curve-fitted to give an entire intensity profile. After the data have been recorded and stored on the PDP, a link is available to transfer the data to a Control Data Corporation Cyber 175 computer for reduction.

The Data Translation A/D board has a maximum sampling rate of 125k samples per second. Thus at this rate, all 16 channels were sampled sequentially in 0.128 ms. In the time delay from sampling the first and last channels (i.e., 0.128 ms) it is possible that some drops will move out of the sample volume and others will move in. Therefore, the results should be considered as an average over this small time window of approximately 0.1 ms. Due to the relatively long transmission lines for the analog signal between the photodetector and the PDP, one scan of the 16 channels was limited to every 0.4 ms. The Data Translation board also has a direct memory access (DMA) interface to move the data to the computer memory as fast as possible. Due to memory limitations on the PDP, a total of 8000 samples can be taken during one run. If all 16 channels are used, then only 500 scans can be taken. Once this is done, the data are written on a disk for permanent storage.

The sampling begins by the PDP receiving a 5-V pulse from the fuel injector pump trigger mechanism which indicates that a fuel injection is about to take place. A block of data is then taken of a predetermined number of scans of the input channels. The computer is put into a wait state until the next trigger pulse is inputted indicating the next fuel injection. This is repeated until 8000 samples are taken. A continuous-running, onboard, real-time clock is sampled each time a scan of the channels is made giving an accurate check of the scan sampling rate.

Computational Analysis

The use of scattered light from particles and particle dispersions has been used by many authors to obtain size and size distribution information. One of the common techniques is to use the light scattered by the particle in the forward direction. If the particle is large compared to the wavelength of light used to illuminate it, the forward-scattered light distribution is dominated by diffraction. In this regime, it can be shown that the forward-scattered light distribution due to a polydispersion is given by

$$\frac{I}{I_0} = \left\{\int_0^\infty \left[\frac{2J_1(\alpha\theta)}{\alpha\theta}\right]^2 N(\alpha)\alpha^4 d\alpha\right\} \Big/ \int_0^\infty N(\alpha)\alpha^4 d\alpha \qquad (1)$$

Here $N(\alpha)$ is the number distribution or the number of particles of average size α per unit range of particle diameter per unit volume of dispersion, where α is a nondimensionalized size parameter. This distribution can, therefore, be obtained from the experimentally determined values of scattered intensity distribution, $I(\theta)$.

In order to obtain the normalized intensity distribution in Eq. (1), the intensity at zero scattering angle, or the centerline intensity I_0, was found by a method suggested by Dieck and Roberts.[11] The scattered intensity profile is extrapolated to zero scattering angle by fitting the existing data (14 points) with a sum of two Gaussian functions. This curve fit was done so that 25 drop size groups could be used instead of 14. The extrapolation to zero scattering angle also provided a convenient normalization parameter for the data and I_0 could be used to find the droplet number concentration in the spray at a later time. Normalization need not be performed on the data but could be postponed until the final drop size distribution. Both normalization techniques result in the same final solution.

Two approaches were taken to the solution of Eq. (1). The first technique gives the results fitted to a known distribution function, while the second was independent of any predetermined distribution. In the first approach, called the iterative distribution fitting method, $N(\alpha)$ is replaced with a chosen distribution function such as a Rosin-Rammler or upper-limit distribution function. Since Eq. (1) is nonlinear, a nonlinear least-squares routine was used to obtain the parameters in the distribution function that give the best values of I/I_0 at every angle at which the intensities are measured.

The second approach, termed the matrix inversion method, use a discretized form of Eq. (1) which is written for each ring of the photodetector. In matrix form, this becomes

$$[J]\ [N] = [I] \qquad (2)$$

Here the $[J]$ matrix is comprised of the Bessel function and its argument, the $[I]$ matrix is the normalized intensity information from intensity profile, and the $[N]$ matrix is the size distribution for each size grouping. Twenty-five size groups were chosen with mean group size ranges from 5 to 125 μm. Each group width was 5μm.

A straightforward matrix inversion of Eq. (2) to find the drop size distribution matrix $[N]$ is not possible due to the characteristics of the equation. Two solution techniques to Eq. (2) have been found in the literature. Ruscello and Hirleman[12] describe a solution using a non-negative least-squares routine. A linear system inversion technique originally developed by Phillips[13] and Twomey,[14] and discussed by Caroon and Borman,[15] has also been a successful solution.

The least-squares method used by Ruscello and Hirleman[12] constrains the drop size matrix to remain positive. The results obtained are in histogram form showing a total number of drops for each size grouping. Unfortunately, it was found that several groups in a row would appear containing no drops; then there would be a large jump in the number of the next group.

The linear system inversion method developed by Phillips[13] and Twomey[14] finds an analytical solution to Eq. (2) by the use of a Lagrange multiplier method. Initially,

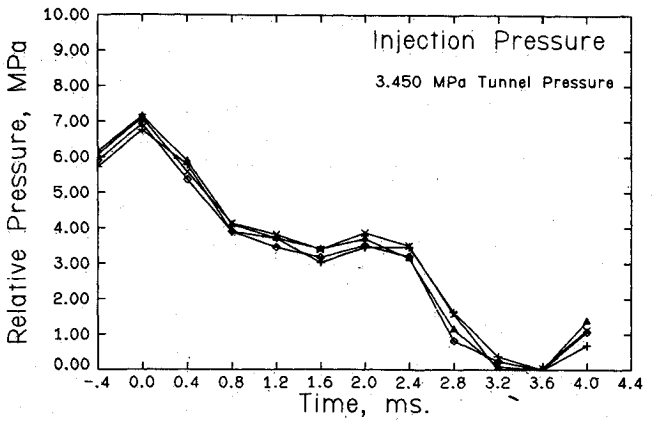

Fig. 4 Fuel-line injection pressure for 0-deg nozzle.

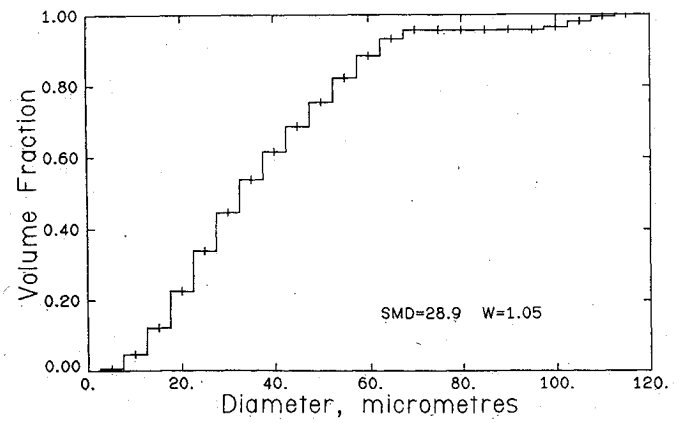

Fig. 3 Typical drop size distribution.

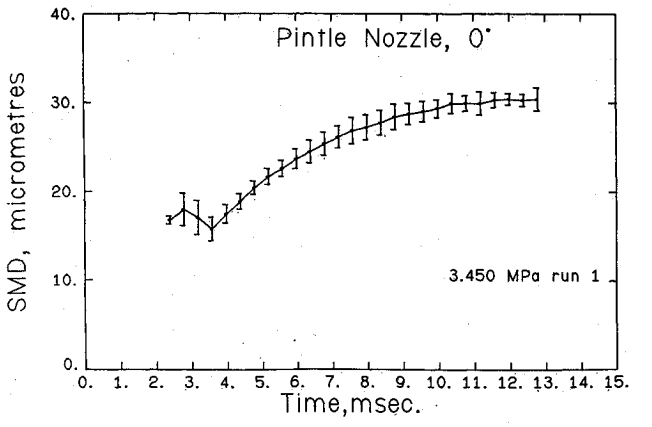

Fig. 5 Plot of average SMD for 12 consecutive cycles.

since the normalized intensity matrix $[I]$ is not known exactly, an arbitrary error matrix is added to the right-hand side of Eq. (2). The system of equations now has an infinite number of solutions. The smoothest solution is chosen, since it is expected that the drop size distribution varies smoothly. It can be shown that the drop distribution matrix is given by

$$[N] = \{[J]^*[J] + \gamma[H]\}^{-1}[J]^*[I] \quad (3)$$

Here $[H]$ is a known constant matrix and γ an undetermined multiplier. As γ is increased, the smoothing of the solution is increased. It should be chosen so that the oscillations are removed, but without appreciably smoothing the solution. The authors found that this was done easily and most accurately by monitoring the number of times the slope of the solution changes sign, and then restricting this to a predetermined number.

After considering all of the preceding solution techniques to Eq. (1), the matrix inversion method was chosen and the matrix equation was solved using the linear system inversion. This produced the most accurate results and did not require the distribution function to be chosen a priori.

Calibration

Several checks were performed on the experimental apparatus to determine the accuracy of the systems. First, a calibration reticle from Laser Electro-Optics, Ltd. was inserted in place of the spray. The calculated results predicted the Sauter Mean Diameter (SMD) to within 4% and the distribution width to within 1% of the manufacturers given parameters.

A test was also performed on the photodetector to check its response to a rapidly changing signal such as the scattered light from a pulsed spray. A chopper wheel was placed in the path of the laser beam and the response of the photodetector was studied using an oscilloscope. All of the rings were analyzed and found to have a similar frequency response. It was found that the rise time from 0 to 95% of full intensity was 0.3 ms.

It was the authors' desire to make measurements as close to the fuel injector as possible to measure the drop distribution that might actually be encountered in a combustion chamber. For the fuel injector used in the spray tunnel, preliminary measurements showed that 2.54 cm from the nozzle was as close as possible without having over 60% attenuation, the maximum attenuation permissible (and still avoid multiple scattering effects), as suggested by Felton.[16] Also from these spray attenuation measurements, it was determined that approximately 10% of the largest spray concentration remained after about 8 ms from the beginning of injection.

Experimental Results

Test Results

The results obtained for the high-pressure tests are reported in terms of the spray SMD and the distribution width. The SMD is defined to be the diameter of a drop which has the same volume-to-surface ratio as the entire spray. Since the forward-scattering method only measures drops passing through the laser beam, the reported SMD is a "line-of-sight" measurement. The distribution width is defined as the difference between the drop size at cumulative volume fractions of 0.8 and 0.2 normalized by the drop size at a cumulative volume fraction of 0.5,

$$\text{Width} = \frac{D_{0.8} - D_{0.2}}{D_{0.5}} \quad (4)$$

A typical size distribution is shown in Fig. 3.

Data were taken at pressures of 0.345, 0.689, 1.38, 2.07, 2.76, and 3.45 MPa in the spray tunnel at a distance of 2.54 cm from the injector tip. At least four runs were taken at each pressure; a run is defined to be 12 consecutive injection cycles. Before the PDP computer began taking data, the pump motor was carefully adjusted and the center ring on the photodetector was monitored for beam attenuation. Care was taken to keep the fuel pump settings the same for all of the runs so that the data could be compared. When the data were compiled, the zero point injection time was defined to be the time when the injection pressure reached a maximum in the fuel line. This time corresponded approximately to the opening of the fuel injector.

The fuel injection pressure was recorded for each of the injection cycles measured. Figure 4 shows a typical pressure trace that was measured for an injection cycle with a tunnel pressure of 3.45 MPa. Plotted is the relative injection pressure for four consecutive cycles in that run. The relative pressure is defined to be the amount above the minimum pressure (arbitrarily set to zero in Fig. 4) in the fuel line for that run. As mentioned before, the actual fuel injector opening pressure is 12 MPa. The similarity seen in these four traces was also seen at all pressures. In fact, all of the pressure traces were similar, between consecutive cycles in a run, between cycles from different runs and between cycles at different tunnel pressures, which indicate that the pump settings for all of the cycles were consistent.

The typical pressure trace in Fig. 4 shows the initial peak pressure which approximates where the fuel injector opens. The primary fuel injection follows until about 2.0 ms after the initial opening, where the line pressure increases again. Here the nozzle opens again to begin the secondary injection period. For all of the cycles analyzed, the primary and secondary injection periods occurred at the same points.

Typical examples of the SMD vs the fuel injection time are shown in Fig. 5. Plotted is the average of 12 consecutive

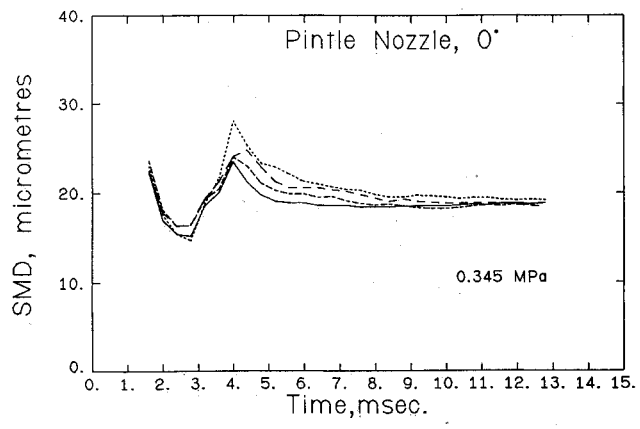

Fig. 6 Plot of SMD for four runs at 0.345 MPa.

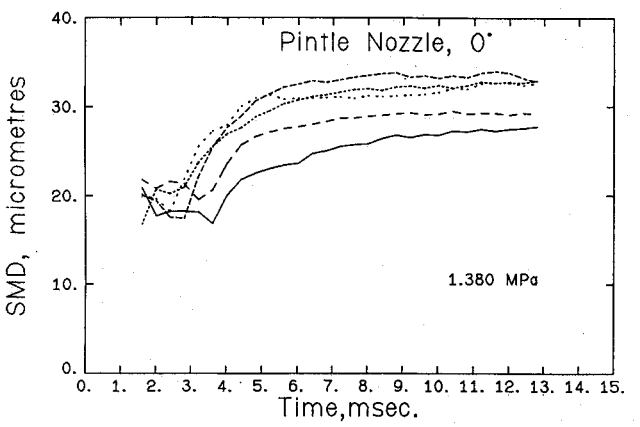

Fig. 7 Plot of SMD for five runs at 1.38 MPa.

cycles, which constitute one run, with error bars of one standard deviation. For each injection pulse, one SMD curve was obtained. These 12 curves (i.e., one run) were then averaged and represented by the solid line. This average illustrates the general trends in the SMD with injection time. The error bars indicate the type of cycle-to-cycle variation that was seen in the SMD. Recall that when using the forward-scattering technique, the resulting mean diameters correspond to the line-of-sight view of the laser beam as the spray passes. Notice that there is a 1.6-2.0 ms delay from when the spray leaves the injector tip to when it reaches the laser beam.

The mean values of the SMD for each run are plotted for some of the tunnel pressures in Figs. 6-8. Each individual curve represents a single run (average of 12 cycles). Except for the runs made at tunnel pressures of 0.345 and 3.45 MPa, all other tunnel pressures had runs (the mean of the 12 consecutive injection cycles) that did not fall within the error bars for a single run. This indicates that there was more variation between random cycles, or cycles from different runs, than between consecutive cycles. For all of the SMD plots, the drop size began to increase at an injection time of 3-4 ms. If these curves are compared to the injection pressure trace in Fig. 4 and the delay of 1.6-2.0 ms from the injector tip to the laser beam is taken into account, this increase in drop size corresponds approximately to the second peak on the pressure trace which indicates the start of secondary injections. Thus the primary injection probably ends at about 3-4 ms on the SMD curves. Therefore, as the injection pressure decreases after the second peak on the pressure trace, the SMD increases as shown at all tunnel pressures (except 0.345 MPa), showing the usual inverse relation between drop size and pressure drop across the injector.

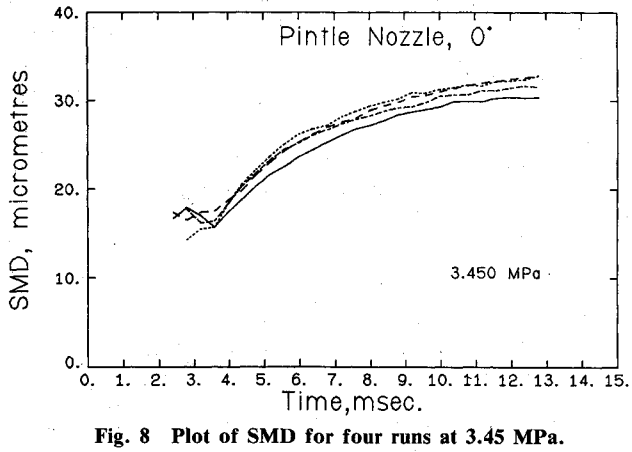

Fig. 8 Plot of SMD for four runs at 3.45 MPa.

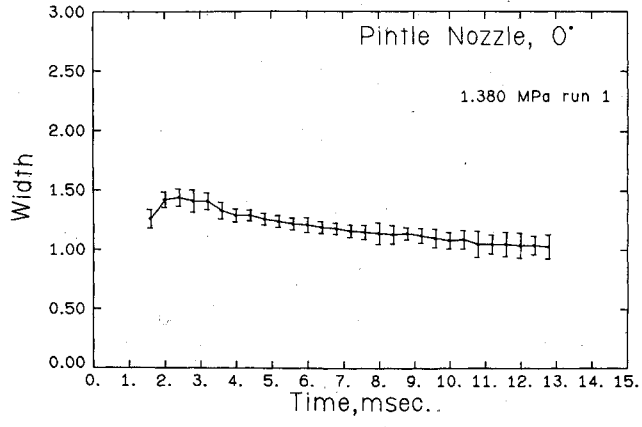

Fig. 9 Plot of average width for 12 consecutive cycles.

For tunnel pressures of 0.689-3.45 MPa, the drop size steadily increases in the secondary injection region. At the high tunnel pressures, the drop sizes in this secondary regime are larger than at lower tunnel pressures. Since the drop size was expected to be inversely related to the pressure drop, the larger drop size was possibly due to the lower pressure drop across the injector at high tunnel pressures.

To see this inverse relationship better, correlations were performed between the average SMD over all of the runs for each tunnel pressure and the pressure drop across the nozzle. Although there was reasonable variation in the correlation coefficient, especially in the primary injection period, the results indicate that in the secondary injection regime the SMD was proportional to the pressure drop across the nozzle to roughly the $-\frac{1}{2}$ power.

The distribution width was also calculated, and a typical plot of width versus injection time is shown in Fig. 9. As with SMD, this plot is the average of 12 consecutive cycles that make up one run and the error bars are one standard deviation. Shown in Figs. 10-12 are the mean widths for each run at each pressure. The widths are relatively large. If, for example, the diameter at a volume fraction of 0.5 is 25 μm (which is possible considering the previous SMD results) and the distribution width is 1.0, this would result in a 25-μm difference between the drop size at a volume fraction of 0.8 and 0.2. This is fairly large, considering the mean size was only 25 μm. However, a large distribution width should be expected with such a large beam diameter (6 mm at $1/e^2$) and so close to the injector tip. Here the beam covers most of the spray diameter, measuring drops throughout the entire spray, resulting in a large distribution width.

Again many of the runs at one pressure exceeded the error bars for a single run, suggesting that the variations between random cycles were greater than between consecutive cycles as found with the SMD.

The trends shown in Figs. 10-12 are opposite those in the SMD. Except for the tunnel pressure of 0.345 MPa, the distribution width decreases with injection time and, for the secondary injection regime, decreases with increasing tunnel pressure. The opposing trends should be expected since the width is inversely proportional to an average diameter [see Eq. (4)]. However, at higher tunnel pressures, there appears to be a lower percentage decrease of the width than percentage increase in the SMD. For example, at a tunnel pressure of 0.345 MPa, the width in Fig. 10 has approximately the same percentage increase as the percentage decrease in the SMD in Fig. 6. However, for a tunnel pressure of 3.45 MPa, the width in Fig. 12 has a substantially smaller percentage decrease than the increase in the SMD in Fig. 8. This suggests that since the distribution width is defined to be the spread in a drop distribution normalized by a mean diameter, the actual spread of the drop sizes tends to become wider with injection time at higher tunnel pressures. How-

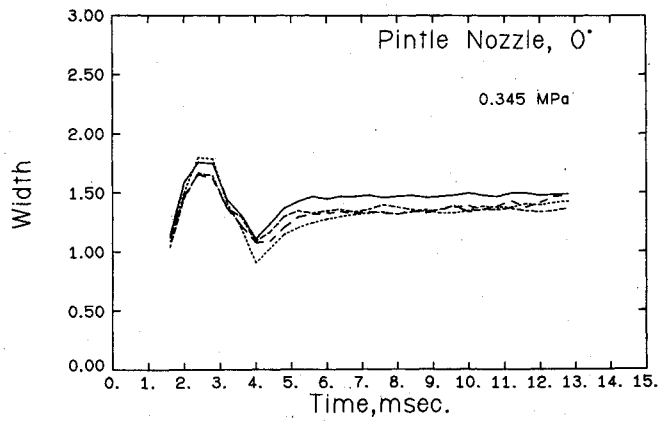

Fig. 10 Plot of width for four runs at 0.345 MPa.

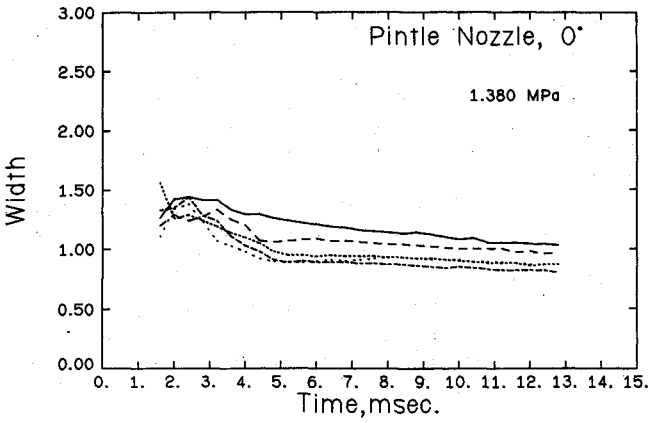

Fig. 11 Plot of width for five runs at 1.38 MPa.

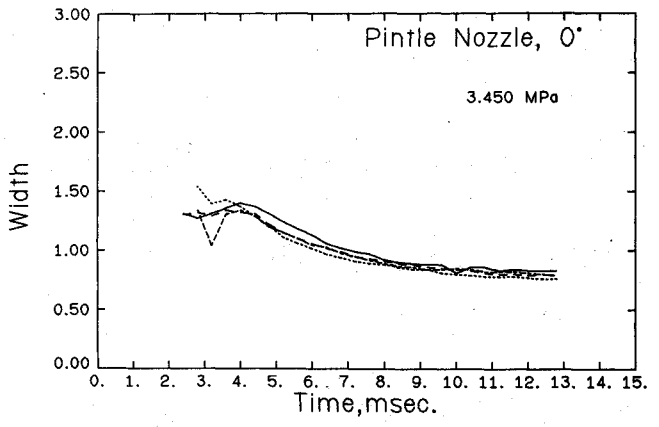

Fig. 12 Plot of width for four runs at 3.45 MPa.

ever, for lower tunnel pressures, the spread in the drop sizes is constant with time since the width is inversely proportional to the SMD trends.

Comparison of Results

Direct comparison to work previously published on pulsed fuel sprays were difficult due to the variations in test conditions between each experiment, e.g., measurement location in the spray and injector type.

The results obtained at low pressure in the spray tunnel (0.345 MPa) can be compared to the general trends of other pulsed spray work at ambient pressures. If only the primary injection period is considered in Fig. 6 (up to 3-4 ms), the trend in the SMD is similar to that found by Hiroyasu et al.[17] Chigier,[6] and Sangeorzan et al.[8] The SMD starts and ends at a large mean diameter and has a minimum between. Also, the spread in the drop sizes appears to be constant since the width in Fig. 10 is inversely proportional to the SMD which agrees with the findings of Sangeorzan et al.[8]

The significant amount of cycle-to-cycle variation found in the spray tunnel results supports our conclusions from tests we have made at ambient pressure. Also, Sangeorzan and coworkers found a greater variation between random cycles than between consecutive cycles for both the SMD and distribution width. Our results agree. Thus, measurement techniques that use several cycles measured at different times and then combine these to form time-resolved information for a single cycle may be misleading. Also, it would require sampling fewer random cycles as opposed to consecutive cycles to obtain good average values of the spray parameters.

Very little published data are available on the effect of elevated pressures on mean size and size distributions in pulsed sprays. However, our results agree with the little that is available. Hiroyasu and Kadota[9] found an increase in SMD with increasing back pressure when using a liquid immersion technique. They indicate that the average SMD over the entire spray increased 20 μm when the back pressure was raised from 0.1 to 5.0 MPa. Takeuchi et al.,[10] using a photomicroscope, showed that during an injection the peak SMD occurred in the middle of the cycle. As the back pressure was raised from 1.0 to 4.0 MPa, there was a 15-μm increase at the middle and end of the injection but less of a change at the beginning. Our results agree in that an approximate 10-μm increase was found in the SMD near the end of the spray pulse as the tunnel pressure was raised from 0.345 to 3.45 MPa. All of these similar results agree that the SMD is, in general, inversely related to the pressure drop across the fuel injector.

The trends found in the distribution width also agree qualitatively with other published results. Hiroyasu and Kadota[9] indicate a general spread in the drop size distribution with increasing back pressure when averaged over the entire spray. As the pressure in the spray tunnel was raised, our results show that the distribution width parameter begins to decrease with injection time. However, as discussed earlier, the SMD increases at a faster rate suggesting that the spread of the drop sizes tended to increase with higher tunnel pressures.

Summary and Conclusions

The following observations can be made as a result of the experimental work contained herein.

1) Detailed time-resolved drop size information has been obtained at varying environmental pressures (up to 3.45 MPa) with the authors' experimental system.

2) Sauter mean diameter (SMD) and drop size distribution information have been found independent of any preselected distribution function for many consecutive and random diesel fuel injection cycles.

3) For a 0-deg pintle nozzle at elevated pressures from 0.345 to 3.45 MPa, both consecutive and random cycles were analyzed.

4) For all elevated pressures except 0.345 MPa, the SMD in the secondary injection region tended to increase as the pressure in the fuel line decreased, suggesting an inverse relationship between drop size and the pressure drop across the nozzle.

5) At elevated pressures the SMD in the secondary injection period increased with increasing environmental pressure, again suggesting an inverse relationship between drop size and the pressure drop across the nozzle.

6) For low environmental pressure (0.345 MPa) the distribution width was inversely proportional to the SMD suggesting a relatively constant spread in the drop sizes during a cycle.

7) As the environmental pressure was raised, the distribution width decreased at a slower rate than the SMD increased indicating a spreading of the drop sizes with injection time at elevated pressures.

8) Significant cycle-to-cycle variation was seen in the SMD and distribution width, however, there appeared to be more cycle-to-cycle variation between random than consecutive cycles.

References

[1]Jones, A. R., "A Review of Drop Size Measurement—The Application of Techniques to Dense Fuel Sprays," *Progress in Energy Combustion Science,* Vol. 3, 1977, pp. 225-234.

[2]Azzopardi, B. J., "Measurement of Drop Sizes," *International Journal of Heat and Mass Transfer,* Vol. 22, 1979, pp. 1245-1279.

[3]McCreath, C. B. and Beer, J. M., "A Review of Drop Size Measurement in Fuel Sprays," *Applied Energy,* Vol. 2, 1976, pp. 3-15.

[4]Hirleman, E. D., "Non-Intrusive Laser Particle Diagnostics," AIAA Paper 83-1514, June 1983.

[5]Swithenbank, J., Beer, J. M., Taylor, D. S., Abbott, D. and McCreath, G. C., "Laser Diagnostic Technique for the Measurement of Droplet and Particle Size Distribution," *Experimental Diagnostics in Gas Phase Combustion Systems,* Progress in Astronautics and Aeronautics Series, edited by B. T. Zinn, Vol. 53, AIAA, New York, 1977, pp. 421-447.

[6]Chigier, N. "Measurement of Droplet Size and Velocity in Pulsed Diesel Sprays," Paper presented at the Eastern Section of the Combustion Institute, Pittsburgh, PA, 1981.

[7]Peters, J. E. and Mellor, A. M., "Pulsed Spray Drop Sizing," *Journal of Energy*, Vol. 5, Jan.-Feb. 1981, pp. 57-59.

[8]Sangeorzan, B., Uyehara, O., and Myers, P., "Time-Resolved Drop Size Measurements in an Intermittent High-Pressure Fuel Spray," SAE Tech. Paper 841361, 1984.

[9]Hiroyasu, H. and Kadota, T., "Fuel Droplet Size Distribution in Diesel Combustion Chamber," *SAE Transactions,* Society of Automotive Engineers, Sec. 3, 1974, pp. 2615-2624.

[10]Takeuchi, K., Senda, J., and Shikuya, M., "Transient Characteristics of Fuel Atomization and Droplet Size Distribution in Diesel Fuel Spray," SAE Tech. Paper 830449, 1983.

[11]Dieck, R. H. and Roberts, R. L., "The Determination of the Sauter Mean Droplet Diameter in Fuel Nozzle Sprays," *Applied Optics,* Vol. 9, No. 9, Sept. 1970, pp. 2007-2014.

[12]Ruscello, L.V. and Hirleman, E. D., "Determining Droplet Size Distributions of Sprays with a Photodiode Array," Paper presented at the Western Section of the Combustion Institute, Paper WWS/CI-81-49, Tempe, AZ, 1981.

[13]Phillips, B. L., "A Technique for the Numerical Soluton of Certain Integral Equations of the First Kind," *Journal of the Association for Computing Machinery,* Vol. 9, Jan. 1962, pp. 84-97.

[14]Twomey, S., "On the Numerical Solution of Fredholm Integral Equations of the First Kind by the Inversion of the Linear System Produced by Quadrature," *Journal of the Association for Computing Machinery,* Vol. 10, Jan. 1963, pp. 97-101.

[15]Caroon, T. A. and Borman, G. L., "Comments on Utilizing the Fraunhofer Diffraction Method for Droplet Size Distribution Measurement," *Combustion Science and Technology,* Vol. 19, No. 5-6, 1979, pp. 255-258.

[16]Felton, P. G., "Measurement of Particle/Droplet Size Distributions by a Laser Diffraction Technique," 2nd European Symposium on Particle Characterization, Nuremberg, 1979, pp. 662-680.

[17]Hiroyasu, H., Toyota, Y., and Kadota, T., "Transient Characteristics of Droplet Size Distribution in Diesel Sprays," University of Hiroshima, Hiroshima, Japan, Jan. 1978.